International Journal of the Physical Sciences Vol. 6(33), pp. 7471 - 7479, 9 December, 2011
Available online at http://www.academicjournals.org/IJPS
DOI: 10.5897/IJPS11.663
ISSN 1992 - 1950 ©2011 Academic Journals

Full Length Research Paper

Study of infusion rate injection profiles on bolus tracking parameters by Monte Carlo simulation

Effat Yahaghi[1]*, Amir Movafeghi[2] and Seyedmahmud Sadatkiai[3]

[1]Department of Physics, Imam International University, Ghazvin, Iran.
[2]Nuclear Science and Technology Research Institute (NSTR), AEOI, P. O. Box 14155-1339, Tehran, Iran.
[3]Nuclear Science and Technology Research Institute (NSTR), Nuclear Science Research School, Tehran, Iran.

Accepted 14 November, 2011

The bolus tracking data are quantified by perfusion and summary parameters when the tissue concentration-time curve and arterial input function vary with the infusion rate injection condition and patient physiology. A new approach based on the Monte Carlo simulation method was used to assess the errors introduced in perfusion summary parameters quantification by difference in injection profiles. The flexibility of the Monte Carlo method allows the employment of the random function for the assessment of arbitrary injection conditions. The results obtained indicate that, the value of each summary parameter investigated is dependent upon both the style and the width of the infusion rate injection profile. As a result, tissue or patient types could easily be incorrectly classified by perfusion and summary parameters. The variations in the patient infusion rate injection profile in the calculations, together with other quantified parameters are presented and discussed in detail.

Key words: Bolus tracking data quantification, Magnetic Resonance Imaging (MRI), summary parameters, perfusion parameters, infusion rate injection profile, Monte Carlo simulation.

INTRODUCTION

In recent years, dynamic contrast enhancement (DCE) MRI has been increasingly used for the measurement of perfusion parameters such as cerebral perfusion (*CBF*), cerebral blood volume (*CBV*), and mean transit time (*MTT*) (Lee et al., 2005; Bahuguna and Petwal, 2010; Ostergaard et al., 1998).

There are two common methods for the quantification of DCE data (Perthen et al., 2002). The first requires measurement of the arterial input function (*AIF*) in order to execute the deconvolution because the concentration of the contrast agent $C_t(t)$ within a region of interest (ROI)) is obtained as the following convolution (Alonzi et al., 2010; Zhao et al., 2008).

$$C_t(t) = \frac{\rho}{k_{II}}(CBF)(C_a(t) \otimes R(t)) \quad (1)$$

where $C_a(t)$ is AIF, that is, the concentration of tracer entering the ROI, and $R(t)$ is the residue function, which describes the fraction of contrast agent remaining in the ROI at time t following the infusion rate injection of an ideal bolus (Dirac-shaped or impulse function) at time *0*. *CBF* is cerebral blood flow, ρ is the density of the brain tissue, and k_{II} accounts for the difference between the hematocrit in the capillaries and large vessels. The physiological parameters *CBF, CBV,* and *MTT* are estimated by this method through a time-consuming deconvolution process. Other researchers use summary parameters calculated directly from the $C_t(t)$ curve (for example, time to peak (*TTP*) and maximum peak concentration (*MPC*), etc) (Zhao et al., 2008; Li et al., 2005; Czosnyka et al., 2004). This method is fast and straightforward and does not require the measurement of *AIF*.

According to Equation 1, the concentration curve measured within the tissue depends not only on the *CBF* within that area, but also upon the particular AIF and $R(t)$

*Corresponding author. E-mail: eyahaghi@ikiu.ac.ir. Fax: (+98) 2813870040. Tel: (+98) 2818371251.

of the region. Variations of the infusion rate injection profile and patient physiology produces different *AIF*s. Also, *R*(*t*) may also vary between patients as well as regionally within the brain (Kim and Kim, 2005; Bihan, 1995). When administering an intravenous infusion rate injection of a contrast agent to a patient, the form of the resulting bolus is very important. The hope is that the infusion rate injection will result in a short and sharp bolus. The ideal case would be a Dirac-shaped or impulse function, so the tissue response can be used as an impulse response (Bihan, 1995). In practice, this ideal case is difficult to approach. Therefore, the injection profiles variations can have an effect on bolus tracking data quantification. In this work, statistical simulations are described in order to study the errors introduced in bolus tracking data and perfusion summary parameters quantification by differences in injection profiles using a new Monte Carlo simulation method. Percentage difference infusion rate injections due to impulse function are determined for summary parameters by simulation. A three-compartment model is used (Yahaghi et al., 2006; Fournier, 1998; Law and Kelton, 1991), and the summary and perfusion parameters are calculated either by a new method based on Monte Carlo simulation and solving the compartmental equations (Yahaghi et al., 2006; Taheri et al., 2011). Nevertheless, the compartmental equations are solved analytically for gamma and impulse input functions, and it is shown that the same results are generated by Monte Carlo simulation. For more complicated inputs, Monte Carlo simulation is used where using the analytical method is too complex to be implemented.

MATERIALS AND METHODS

The compartmental model

The Tofts and Kermode's compartmental model (TKM) (Tofts and Kermode, 1991) is used for the study of infusion rate injection profiles on bolus tracking parameters. TKM consists of four compartments: a plasma space, an extracellular space, a drain space and a leakage space. The modified TKM consists of three compartments: A plasma space, a drain space and a tissue and is displayed in Figure 1. It is assumed that the particles of the contrast agent remain in the capillary of the tissue and do not diffuse to extravascular space. In the model, the plasma space is connected to the tissue. The drain space removes the contrast agent from the plasma space. A bolus of contrast agent is injected to the plasma at time *t=0* s. Fast mixing is assumed within the plasma and other compartments. According to the mass conservation law, flow from plasma to the tissue and the drain space is obtained using the mass balance in Equation 2:

$$-V_p \frac{dC_p(t)}{dt} = K_1(C_p(t) - C_t(t)) + K_2 C_p(t) \qquad (2)$$

where $C_p(t)$ is the contrast agent concentration in the plasma space

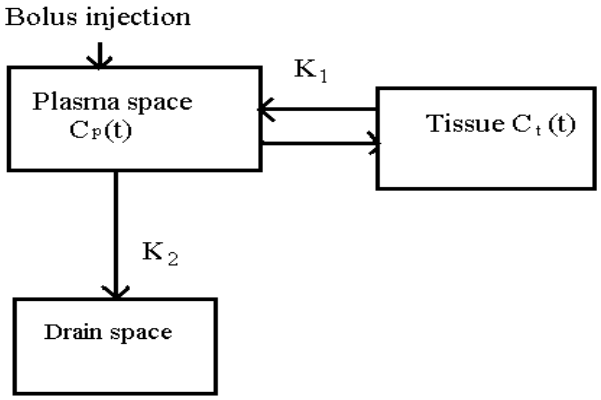

Figure 1. The modified compartmental model consisting of three compartments: Plasma, tissues and drain space.

(*mM/l*), K_1 and K_2 are constants describing the flow rate per unit concentration difference (ml/min), V_p is plasma volume, and $C_t(t)$ is the contrast agent concentration in tissue (*mM/l*). In this simulation, patient physiology is supposed to be invariant and only the infusion rate injection profile is considered to be variable. So K_1 and K_2 will have the same value in all investigated cases in this study.

Also, the relationship between the flow and tissue is described by Equation 3:

$$-V_t \frac{dC_t(t)}{dt} = K_1(C_t(t) - C_p(t)) \qquad (3)$$

where V_t is the volume of the tissue. These units are according to Tofts et al. (1999) finding. By solving Equations 2 and 3, the concentrations of the contrast agent in plasma and tissue as a function of time can be derived. Note that Equations 1 and 2 are similar when *R(t)* is an exponential function and $C_p=(1-Hct)C_a$.

For each of the contrast agent concentration-time curves, the more commonly used summary and perfusion parameters can be calculated. The expansion formulae of *ITP* (Integral To Peak), *MTT*, *CBF* and *CBV* are as follows in Equation 4 (Perthen et al., 2002; Bihan, 1995; Yahaghi et al., 2006) (Figure 2):

$$ITP = \int_0^{TTP} C_t(t)dt \Big/ \int C_a(t)dt \qquad (4)$$

Normalized first moment; $MTT = \int_0^T tC_t(t)dt \Big/ \int_0^T C_t(t)dt$, referred to as "*MTT*" since this measure is commonly used as a quantitative approximation to *MTT*. Two perfusion index *CBF=CBV/MTT, and*

$$CBV = \int C_t(t)dt \Big/ \int C_a(t)dt .$$

Transfer time from one compartment to other compartments

Crossing of particles from one compartment to the others could be considered as a simple weighted summation of exponential decay

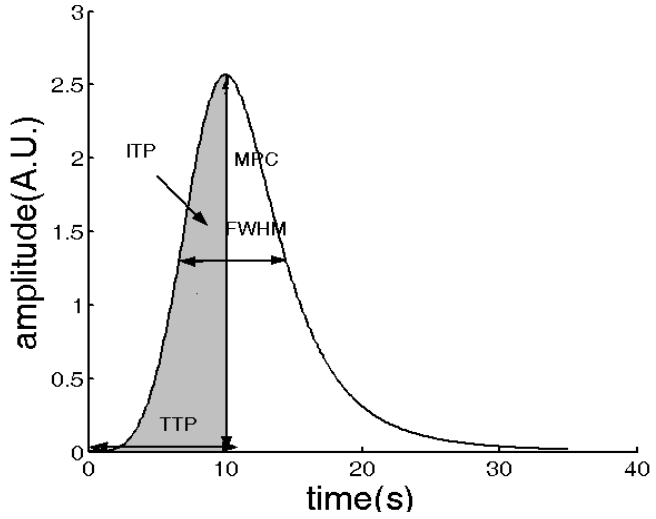

Figure 2. Schematic tissue concentration-time curve illustrating summary parameters.

by independent models (Fournier, 1998). The number of particles in each compartment follows the exponential function as Equation 5:

$$C_i(t) = A_i \exp(-\lambda_i t) \quad (5)$$

where *i* refers to plasma and tissues, λ_i is the rate constant of each compartment, and A_i is the amplitude component. The probability of exiting from a compartment and entering to another compartment in the time interval *dt* is shown by Equation 6:

$$P_i(t) = \lambda_i \exp(-\lambda_i t)dt \quad (6)$$

and the related distribution function is written as Equation 7:

$$S_i(t) = \int_0^t P_i(t)dt = 1 - \exp(-\lambda_i t) \quad (7)$$

From which the inverted function can be obtained as Equation 8:

$$S_i^{-1}(t) = t_t = \frac{-\ln(\xi)}{\lambda_i}, \qquad 0 \le \xi < 1 \quad (8)$$

where *i=p,t* refers to plasma and tissues, t_t is time of transit from one compartment to another compartment, λ_i is the rate constant, and ξ is a uniform random variable distributed between (*0-1*) (Law and Kelton, 1991).

Implemented methods

Two methods of calculations, $C_p(t)$ and $C_t(t)$ are presented, The Monte Carlo simulation and the analytical method. For the determination of $C_p(t)$ and $C_t(t)$, the following cases are employed: For the case (a), the compartmental model with bolus infusion rate injection (impulse function) and gamma-variate input function, and for the case (b) the compartmental model with box, trapezoidal and random input functions.

For the first case, the compartmental model is analytically solved using MATLAB software due to its feasibility and flexibility. The Monte Carlo simulations are used for the second case due to the complexity of solving the compartmental equations with box, trapezoidal and random inputs, because analytical solution in the compartment equations is a complicated task to tackle.

Monte Carlo simulation

The Monte Carlo simulation is based on the movements of the contrast agent particles between the three compartments. Particles enter the plasma compartment at specific times and move to other sections according to the rate constant K_1 and K_2. It must be mentioned that K_1 and K_2 are related to patient physiology and are constant. A fraction of the particles stay in the plasma space and the rest go to other compartments, but many of the particles will return to the plasma space. The ratio of the particles that go out from each compartment to the initial particles in the compartment must be calculated at an interval of time. For the simulation, the coefficients of the particles that have moved to other compartments are calculated according to compartmental Equations 2 and 3 by Equations 9:

$$\lambda_{p-t-d} = \frac{K_1 + K_2}{V_p}, \qquad \lambda_{t-p} = \frac{K_1}{V_t}$$

where the coefficients of $\lambda_{p\text{-}t\text{-}d}$, $\lambda_{t\text{-}p}$, are used for calculating the particles exited from the plasma space and the tissue, respectively and *t*, *p* and *d* indices referred to tissue, plasma and drain.

The particle transfer time from one compartment to another compartment is calculated by Equation 8. Besides, the transfer time has to be compared with a reference time of particle diffusion which is called random walk time. The average time of random walk or travel path along one direction is described by Einstein as Equation 10 (Bihan, 1995):

$$\Delta t = L_D^2 / 2(ADC) \quad (10)$$

where *ADC* is the apparent diffusion coefficient (usually given in cm^2/s or mm^2/s) and Δt is the observation time (s). The Δt is set to 40 ms, *ADC* to 8×10^{-6} cm^2/s and L_D, the average displacement along one direction becomes 9 *μm* (Bihan, 1995).

For the simulation, we consider that the particles of the contrast agent enter the plasma with a bolus infusion rate injection like impulse function, and for the calculation of the contrast agent concentration in each compartment, the ratio of N_{exited} to $N_{initial}$ is evaluated for each compartment. For the calculation of this ratio, the value of λ is found from Equation 9 and for t_t from Equation 8. Then a random number ξ is generated with a uniform distribution between 0 and 1. If the values of t_t are between 0 and Δt, then the contrast agent particle will move out to the other compartment, and, otherwise, in the case that the t_t values are larger than Δt, the particle will stay in this compartment. The particles movements are followed and their position and time are registered in each step. 2×10^{-4} trajectories are generated for each *dt* in the simulation (Number of trajectories are related to the statistical error which will be explained subsequently). Then the ratios of N_{exited} to $N_{initial}$ are calculated in a time interval for each compartment. The concentration of the particles in plasma is calculated by Equation 11:

$$C_p(t_i) = (1 - \frac{N_{exited-p}}{N_{initial-p}})C_p(t_{i-1}) + \frac{N_{exited-t}}{N_{initial-t}}C_t(t_i) + r(t_i) \quad (11)$$

where $r(t_i)$ is the input of the plasma and is zero at time $t=0^-$. According to this equation, the concentration contrast agent of the plasma compartment in a time interval is the sum of the remained particles and those which come from the tissue. Likewise, the concentration in tissue is obtained as Equation 12:

$$C_t(t_i) = (1 - \frac{N_{exited-t}}{N_{initial-t}})C_t(t_{i-1}) + \frac{N_{exited-p}}{N_{initial-p}}C_p(t_i) \quad (12)$$

The tissue has no input. Finally, to calculate the statistical error in the crossing of the particles, the mean value of the crossing from one compartment to another compartment is obtained by Equation 13:

$$\bar{x} = \frac{\sum_{i=1}^{n} f_i x_i}{n} \quad (13)$$

where f_i is abundance of each particle, which is 1. In our case, x_i is the probability of the particle crossing from one compartment and can take values of 0 or 1, and n is total particles in a compartment. The standard deviation of the crossing from a compartment is calculated by Equation 14:

$$\sigma = \sqrt{\frac{\sum_{i=1}^{n} f_i (x_i - \bar{x})^2}{n(n-1)}} \quad (14)$$

and the relative percentage error is found by Equation 15:

$$\bar{S} = \frac{\sigma}{\bar{x}} \times 100 \quad (15)$$

Finally, different programs in MATLAB environment are executed for the implementation of each algorithm.

RESULTS

To obtain the results, patient physiology and $R(t)$ of the brain are assumed constant and the effect of the infusion rate injection profile on the summary parameters are investigated.

Validity of Monte Carlo simulation using the analytical method and Wienmann data

The compartmental model is considered with three compartments; the plasma space, the tissue and the drain space. A bolus of Gd-DTPA is injected into the plasma. Fast mixing is assumed within the plasma and other compartments. The analytical method and the Monte Carlo simulation are used for calculating $C_p(t)$ and $C_t(t)$. The concentration of the contrast agent at time $t=0^-$ is zero in all compartments except the plasma space. The concentration of the plasma is equal to the dose at initial time divided by the volume of plasma. The results of the Monte Carlo simulation, the analytical method, and the data of Weinmann (Tofts and Kermode, 1991) for the plasma space are displayed in Figure 3.

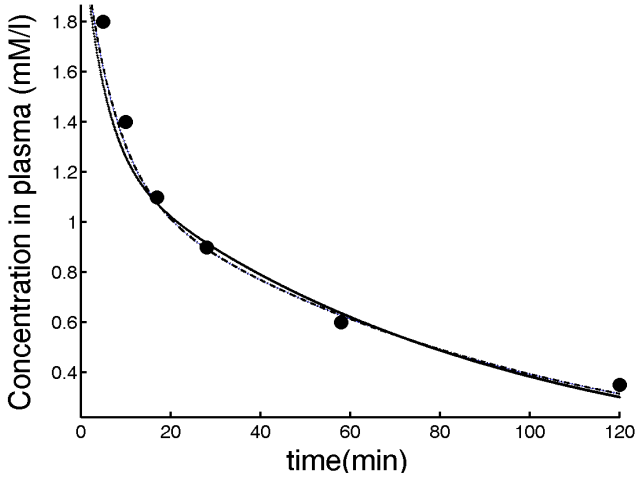

Figure 3. The concentrations of the contrast agent in plasma are derived by solving the compartmental equations and Monte Carlo simulation (solid line) with bolus infusion rate injection as the plasma input. Agreement of Monte Carlo results with the Weinmann datablack circle) and results of analytical method (dashed line) can be observed.

According to Figure 3, the peak contrast agent concentration in the plasma space appears at time zero and then decreases exponentially as the time increases. As one can see, the results of the Monte Carlo simulation and the analytical method agree very well with the Weinmann data. The concentration of contrast agent in tissue as a function of time is shown in Figure 4. The concentration of the contrast agent increases in tissue from zero to a maximum value and then decreases slowly as the fresh blood enters the plasma and other space, washing out the contrast agent from the tissue. The relative statistical errors are calculated by Equations 12 to 14. The value of relative statistical errors depends on the number of particles, however the number is more, and so the error is lower. The mean values of the relative statistical errors for $C_p(t)$ and $C_t(t)$ are obtained as 0.95 and 0.94%, respectively.

Validity of Monte Carlo simulation using analytical method for the gamma variate function as input

In this case, an arbitrary gamma variate function is considered as the input of the plasma space and the occurrence of its peak value is assumed to appear at the time $t=3$ s. The concentration of the contrast agent in all

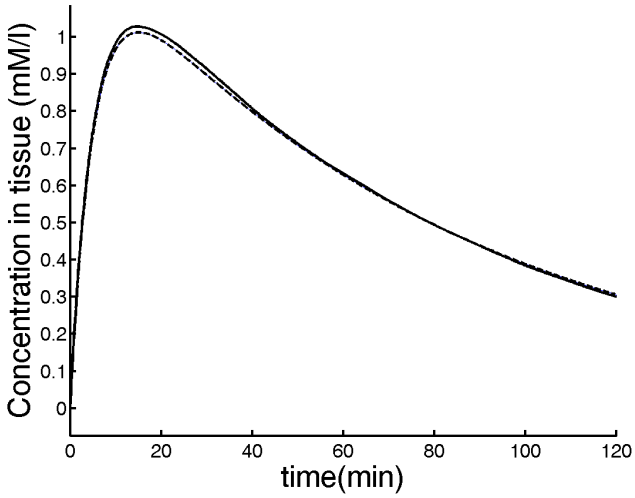

Figure 4. The concentration of contrast agent in the tissues space versus time with bolus infusion rate injection as the plasma input by solving the compartmental equations (solid line) and Monte Carlo simulation (dashed line).

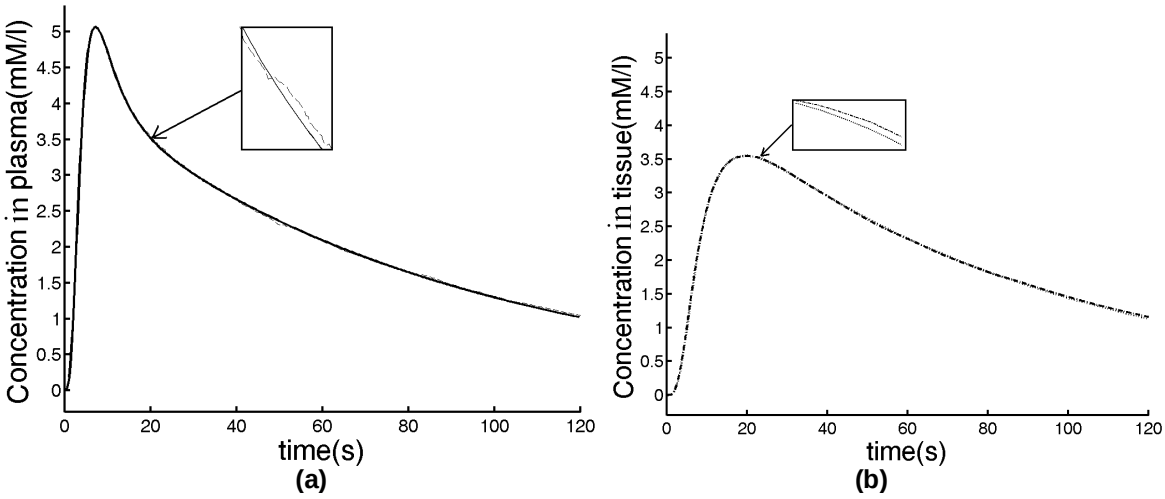

Figure 5. (a) The contrast agent concentration of the plasma space versus time are obtained by solving the compartmental equations (solid line) and Monte Carlo simulation (dash-dot line); (b) The contrast agent concentration of the tissue versus time are obtained by solving the compartmental equations (dashed line) and Monte Carlo simulation (dotted line) with gamma variate function as the plasma input. The parts of curves are shown in different scale.

compartments are zero at time *t=0.* The infusion rate injection enters the plasma compartment and then particles enter other compartments proportional to K_1, *and* K_2. Figure 5 shows the result of the contrast agent concentration of plasma space, Figure 5a and tissue, Figure 5b. The plasma and tissue concentration contrast agent increases proportional to the infusion rate injection function, reaches a peak, and then decreases slowly as fresh blood enters the plasma space, washing out the contrast agent. The mean values of the relative statistical errors of $C_p(t)$ and $C_t(t)$ are 0.24 and 1.22%, respectively. These results are obtained using the Monte Carlo simulation method and by solving the compartmental equations. The results of the Monte Carlo simulation method; Figure 5a and b coincide well with analytical results obtained from solving the compartmental equation.

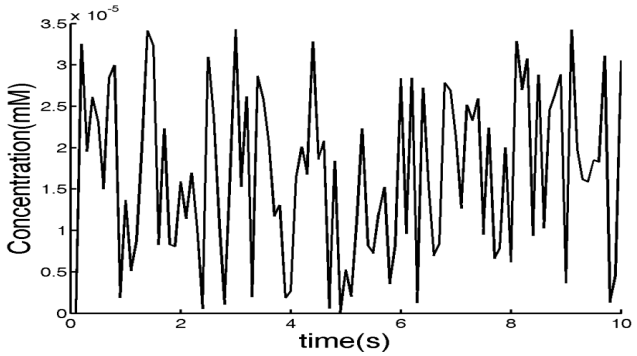

Figure 6. A type of used random function as infusion rate injection input function. The amplitude of function is random and its width is 10 s.

This shows that the Monte Carlo method is capable of generating precise results. Therefore, this method can be used for some other complex input functions.

Results of Monte Carlo simulation for box, trapezoidal and random functions as input

Here, it is assumed that the infusion rate injection function has a different style like box, trapezoidal and, finally, it is considered as a random function. A profile of the random function is shown in Figure 6. The width of all three input functions is chosen to be between 1 and 10 s in ten successive steps and they are considered as the input of the plasma space with different widths. The area under these functions or the dose of each infusion rate injection is constant and equal, only their widths and styles are different.

The concentration of contrast agent in all compartments is zero at time *t=0* for each simulation. The input infusion rate injection function enters the plasma compartment, and particles of the contrast agent enter other compartments proportional to K_1 and K_2. Also, the concentrations of the contrast agent are obtained over time in the plasma and the tissue by the Monte Carlo simulation. The widths of functions are taken between 1 and 10. For each of the resulting simulated contrast agent concentration-time curves, the more commonly used summary and perfusion parameters are calculated. The summary parameters are calculated for the simulated curves and the variations of summary parameters with respect to the infusion rate injection width are also investigated for box, trapezoidal and random function. In Figure 7, we show the summary parameters variation as a function of the infusion rate injection width for some of the results.

The error bars shown in Figure 7 are the maximum values of the relative statistical errors which are negligible on some curves like the *MPC* of plasma such as Figure 7a. The simulation results show that *MPC* and *ITP* depend on the style of infusion rate injection like Figure 7a and b, but the summary and perfusion parameters are almost independent of styles of infusion rate injection such as *TTP,* full width at half maximum (*FWHM*) of plasma, *FWHM* of tissue and *MTT* like Figure 7c to f.

The results of simulation obtained in this work indicate that all of the summary parameters vary with the width of the infusion rate injection function. The variations of the plasma parameters ascend to infusion rate injection width such as *TTP* and *FWHM* of plasma, Figure 7c and d; except for the plasma *MPC*. Also, the variation of tissue parameters is descending as in the case of the *ITP* and *FWHM* of tissue, Figure 7b and e; except in the tissue *MPC*. The presented results show that the *TTP* of tissue is not only independent to the style of the infusion rate injection, but also, it is dependent on the width of infusion rate injection. Most of the parameters shown in this work are greatly varied over the infusion rate injection width range such as the *TTP* of plasma, the *FWHM* of tissue and *MTT*. The variation ranges of the summary parameters are considerable. For example, in the case of the *FWHM* of plasma; this variation is usually between 4.5 and 8.7 s for the trapezoidal function as shown in Figure 7d. For each parameter, the impulse infusion rate injection is considered as an ideal infusion rate injection and its variation can be estimated as the most and least relative difference percentages with respect to the impulse function. The maximum and the minimum of the relative difference percentages of summary and perfusion are shown in Table 1. The relative differences for *TTP* and *ITP* of plasma are not calculated in the case of the impulse function because of being divided by zero error. The relative differences for some of the parameters are highly dependent on the width and style of the infusion rate injection function (Table 1). For example, the *MPC* of the plasma relative differences are between 22.7and 43.8% for the box functions and between 15.17 and 30.7% for the trapezoidal functions. The *MTT* has the lowest percentage variation over the infusion rate injection range, having a percentage variation of between 0.115 and 8.24% for random function.

DISCUSSION

This work studies effect of infusion rate injection profiles on bolus tracking parameters by Monte Carlo simulation. In all cases, it is assumed that the contrast agent concentration is zero throughout the each compartments at time t = 0 and the contrast agent as infusion rate injection enters the plasma at x = 0. The contrast agent moves through the plasma with time and enters the other compartments depending on the assumed flow rate of each compartment.

The compartmental model is analytically solved

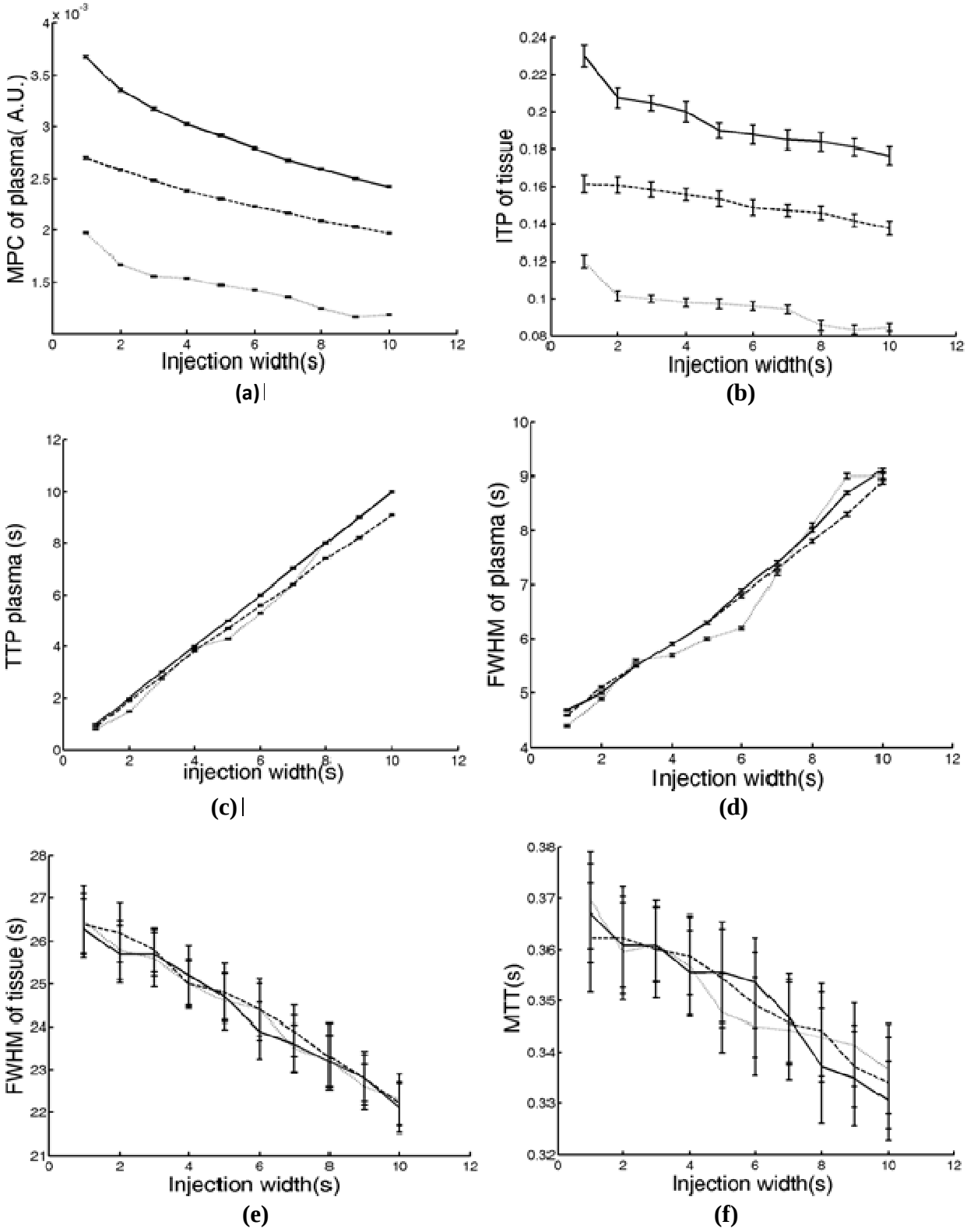

Figure 7. Variations of the summary and perfusion parameters of plasma and tissue versus width of infusion rate injection for the variations of the infusion rate injection profile (box function (the solid curves), trapezoidal function (the dashed curves) and a random function (the dotted curves)): (a) *MPC* of plasma, (b) *ITP* of tissue, (c) *TTP* of plasma, (d) *FWHM* of plasma, (e) *FWHM* of tissue, and (f) *MTT*.

Table 1. Variations of the summary and perfusion parameters with the variations of the infusion rate injection profile.

Percentage difference with respect to impulse function		*MPC* (A.U.) (%)	*TTP* (s) (%)	*FWHM* (s) (%)	*ITP* (s) (%)	*CBV* (ml/g) (%)	*CBF* (ml/s/g) (%)	*MTT* (s) (%)
Box function	*Cp(t)*	22.7-43.8	-	0.5-119	-	1.4-9.2	2.24-16.4	0.77-8.67
	$C_t(t)$	21.1-23.1	0	1.4-17.2	14.8-31.7			
Trapezoidal function	*Cp(t)*	5.17-30.7	-	11.9-116.6	-	0.46-8.49	0.29-5.6	0.7-0.5
	$C_t(t)$	0.28-12.2	0	0.74-16.4	0.07-12.7			
Random function	*Cp(t)*	43.6-.66.1	-	4.7-114.2	-	0.21-10.1	0.71-17.1	0.51-8.46
	$C_t(t)$	41.8-52.6	0	1.1-16.8	33.6-59.8			

and the Monte Carlo simulations are used for solving the compartmental equations with box, trapezoidal and random inputs, because analytical solution in the compartment equations is a complicated task to tackle (Yahaghi et al., 2006).

Then the summary parameters are calculated for the simulated curves and the variations of summary parameters with respect to the infusion rate injection width are also investigated for box, trapezoidal and random function. The results is shown that for small width of infusion rate injection, *MTT, CBF and CBV* have a negligible percentage of relative variation and can be used for the estimation of the abnormalities in the tissue with less error. Some of the other summary parameters vary significantly with the infusion rate injection profile as *MPC* of plasma and tissue, and thus are not suitable in practice for quantification of tissue abnormalities.

The flow rate of each compartment depends on several parameters such as the solute diffusivity, pore area, the total surface, thickness of membrane, an experimental parameter tortuosity, partition coefficient, and radius of pore. The variations of these parameters can affect the concentration of the contrast agent and summary parameters. These can be investigated by the Monte Carlo simulation (Kim and Kim, 2005; Yahaghi et al., 2006).

The results obtained for many different sets of box, trapezoidal and random functions as input show that, in general, the referencing of summary and perfusion parameters does not eliminate the differences caused by variations in the infusion rate injection profile. This outcome could not be achieved simply in an analytical solution for the compartmental model. Nevertheless, this method has to be considered further in future studies.

A disadvantage of the method is its long execution time, especially when a large number of particles are used for reducing the error. These calculations are usually done off-line and thus the execution speed is not critical. However, on-line determination has its own advantages; therefore, fast computing methods such as parallel computing may be used (Law and Kelton, 1991).

CONCLUSION AND RECOMMENDATION

This work concerns the use of the statistical Monte Carlo method which allows one to determine the effect of infusion rate injection profiles on summary parameters in plasma space and tissue by compartmental model. In this approach, we are not dealing in solving complicated equations, so some new parameters can be considered in the models by probability density functions, and any arbitrary nonlinear functions and infusion rate injection effects can be studied. This study shows that all of the summary parameters are dependent on the infusion rate injection profile, but not in the same order. Ideally, parameters that are independent of patient infusion rate injection type and width are required, but this was not the case for any of those tested in these simulations.

In future studies, the simulation could be used to assess the effects of cardiac output and vascular structure as a mathematical function on perfusion and summary parameters.

Also, the presented study can be used for investigating the effect of extravascular exchange of tissue as a compartmental model with a different infusion rate injection. The effect of contrast agent and tissue parameters such as the solute diffusivity, pore area, the total surface, the thickness of the membrane, an experimentally

parameter tortuosity, partition coefficient and radius of pore on summary parameters and extravascular contrast agent exchange can be investigated by the model without solving complicated equations (McCommis et al., 2008; Tofts et al., 1999; Kim et al., 2011).

REFERENCES

Lee MlC, Cha S, Chang SM, Nelson SJ (2005). Dynamic susceptibility contrast perfusion imaging of radiation effects in normal-appearing brain tissue: Changes in the first-pass and recirculation phases. J. Magn. Reson. Imaging., 21**:** 683–693.

Bahuguna SK, Petwal KC (2010). Spatial transformations of diffusion tensor magnetic resonance imaging using certain geometric operations. Int. J. Phys. Sci., 5(7): 940-954. Available online at http://www.academicjournals.org/IJPS

Ostergaard L, Smith DF, Vestergaard-Poulsen P, Hansen S B, Gee AD, Gjedde A, Gyldensted C (1998). Absolute cerebral blood flow and blood volume measured by magnetic resonance imaging bolus tracking: comparison with positron emission tomography values. J. Cereb Blood Flow Metab., 18: 425–432.

Perthen JE, Calamante F, Gagian DG, Conelly A (2002). Is quantification of bolus tracking MRI reliable without deconvolution. Magn. Reson. Med., 47(6): 61-67.

Alonzi R, Taylor NJ, Stirling JJ, d Arcy J A, Collins DJ, Saunders MI, Hoskin PJ, Padhani AR (2010). Reproducibility and correlation between quantitative and semiquantitative dynamic and intrinsic susceptibility-weighted MRI parameters in the benign and malignant human. prostate. J. Magn. Reson. Imaging, 32: 155–164.

Zhao L, Sukstanskii AL, Kroenke D, Song J, Piwnica-Worms D, Ackerman JJH, Neil JJ (2008). Intracellular Water Specific MR of Microbead-Adherent Cells: HeLa Cell Intracellular Water Diffusion", Magn. Reson. Med., 59: 79-84.

Li X, Rooney WD, Springer ChS (2005). A unified MRI pharmacokinetic theory: intravascular and extracellular contrast reagents. Magn. Reson. Med., 54(6): 1351-1359.

Czosnyka M, Czosnyka Z, Momjian Sh (2004). Cerebrospinal fluid dynamics. Physiol. Meas., 25 R51-R76. PII: S0967-3334 (04).

Kim T, Kim SG (2005). Quantification of Cerebral arterial blood volume and cerebral blood flow using MRI with modulation of tissue and vessel (MOTIVE) signals. Magn. Reson. Med., 54: 333–342.

Bihan DL (1995). Diffusion and perfusion magnetic resonance imaging: Applications to Functional MRI. New York: Raven Press, ISBN: 205-211. 0-7817-0244-5.

Yahaghi E, Soltanian-Zadeh H, Shahriarei M, Fatouraee N, Ewing JR (2006). Estimation of Contrast Agent Concentration in Intra- and Extra-Vascular Spaces of Brain Tissue. Math. Bio., 204:102–118.

Fournier RL (1998). Basic transport phenomena in biomedical engineering. London Taylor and Francis. ISBN:1-560-32-708-1; pp. 115-144.

Law AM, Kelton WD (1991). Simulation modeling and analysis New York: McGraw-Hill. Pp. 240-278.

Taheri S, Gasparovic Ch, Shah NJ, Rosenberg GA (2011). Quantitative measurement of blood-brain barrier permeability in human using dynamic contrast-enhanced MRI with fast T1 mapping , Mag. Reson. Med., 65(4): 1036–1042.

Tofts PS, Kermode A (1991). Measurement of blood brain barrier permeability and leakage space using dynamic MR Imaging 1. fundamental concepts. Magn. Reson. Med., 17**:** 357-367.

McCommis KS, Zhang H, Herrero P, Gropler RJ, Zheng J (2008). Feasibility study of myocardial perfusion and oxygenation by non-contrast MRI: comparison with PET study in a canine model. Magn. Reson. Imaging. 26: 11– 19.

Tofts PS, Brix G, Buckley DL, Evelhoch JL, Henderson E, Knopp MV, Larsson HBW, Lee T-Y, Mayr N A, Parker GJM, Port RE, Taylor JS, Weisskoff RM (1999). Estimating kinetic parameters from dynamic contrast-enhanced T1-weighted
MRI of a diffusible tracer standardized quantities and symbols. Magn. Reson. Med., 10: 223–232.

Kim KA, Kim GlHM, Chung YE, Hong H-S, Choi SY (2011). Three-dimensional contrast-enhanced hepatic MR imaging: Comparison between a centric technique and a linear approach with partial Fourier along both slice and phase directions. J. Magn. Reson. Imaging. 33(1): 160–166.